ISSN 2303-4521
PERIODICALS OF ENGINEERING AND NATURAL SCIENCES
Vol. 1 No. 1 (2013)
Available online at: http://pen.ius.edu.ba

Modulated (Spinodal) Alloys

Fehim Findik

International University of Sarajevo,
Faculty of Engineering and Natural Sciences,
Address: Hrasnička cesta 15,
71210 Ilidža, Sarajevo
Bosnia&Herzegovina
E-Mail: ffindik@ius.edu.ba

Abstract:
In this work, after defining spinodal reactions experimental investigation on spinodal decomposition are overviewed for the last five decades. Also, future developments in spinodal decomposition for modulated alloys are forecasted and criticized in an outlook.

Keywords: multi-materials; castings; microstructure

1. INTRODUCTION

Spinodal decomposition is a clustering reaction and as a result of this reaction homogeneous, supersaturated, solid or liquid solution splits suddenly into two phases. The twin phases produced by the spinodal decomposition of a supersaturated solid solution differ in composition from the parent phase, but have basically the same crystal structure. The physical implication of the spinodal is that it is the border between the unstable and metastable parts of a two phase region. This can be established by formative the sign of the alteration in free energy for a little composition fluctuation.
decompose into two phases along two dissimilar reaction paths [1].

The phase transformation that can produce a spinodal reaction object is decomposition within a stable or metastable miscibility gap (Fig. 1). If a solid solution of composition C0 is solution treated in the single-phase field at a temperature T0, then aged at an intermediate temperature TA (or TA'), the single-phase alloy subjects to separate into a two-phase mixture. At the temperature TA, the compositions of the twin phases α_1, and α_2 under equilibrium conditions are C1 and C2, correspondingly. Nevertheless, the supersaturated solid solution may

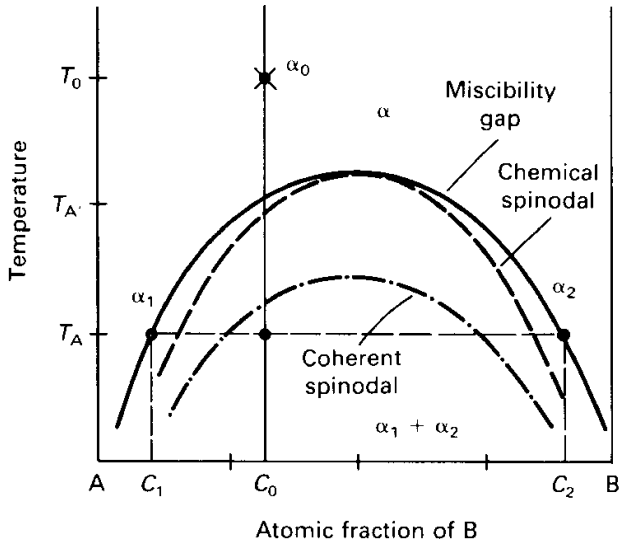

Figure 1 – Schematic showing miscibility gap in the solid state and spinodal lines (chemical and coherent) [1]

DOI: 10.21533/pen.v1i1.16

At small undercoolings or low supersaturations (TA'), the solution is metastable; exterior of a second phase engages comparatively large restricted composition changes. This is the classical nucleation procedure, giving rise to "critical nuclei," which can expand suddenly. As the particles of the newest phase expand by diffusion, the matrix composition regulates in the direction of equilibrium. At large supersaturations (TA), the solution is unstable, and the two-phase mixture gradually emerges by the enduring enlargement of mainly small amplitude changes (Fig. 2). The rate of reaction is directed by the rate of atomic migration and the diffusion distances concerned, which depend upon the scale of decomposition (undercooling). Therefore, spinodal structures relate to phase mixtures that attain from a kinetic procedure leading the early stages of phase separation. The "spinodal line" revealed in Fig. 1 is not a phase boundary but a separation representing a difference in thermodynamic stability [1, 2].

In the current work, the advantages of spinodal decomposition, experimental investigations on modulated (spinodal) Cu-based alloys, and future developments in spinodal decoposition are reviewed.

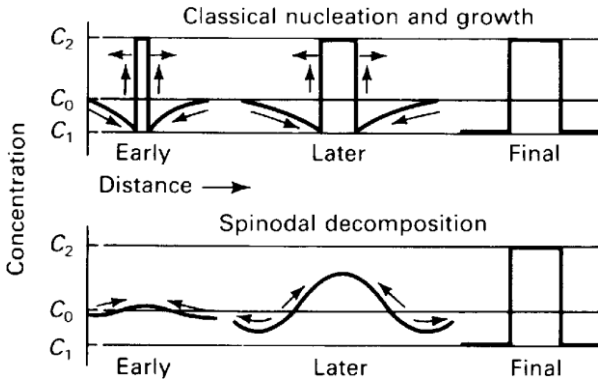

Figure 2 – Schematic illustrating two sequences for the formation of a two-phase mixture by diffusion processes: nucleation and growth and spinodal decomposition [2]

2. ADVANTAGES OF SPINODAL DECOMPOSITION

Precipitation hardening, dispersion strengthening and spinodal decomposition methods provide almost the identical strength values. Conversely there are definite advantageous of using spinodal decomposition process as against the precipitation hardening method. These are abridged here [3]:

a) The decomposition-product phases have the identical structure but are dissimilar in composition, while in the case of precipitation the precipitate phase has a unlike structure and composition from that of the matrix. The principal advantage of the products having the identical structure is that microstructure is consistent. Consequently there are no local anodes and cathodes (eg grain boundary precipitates) to deteriorate corrosion resistance.
b) In spinodal decomposition, there is no nucleation barrier and thus there is no need to offer activation energy. Therefore, hardening by spinodal decomposition is not predisposed by section thickness or quenching rate. Though, in the case of precipitation hardening, there is a nucleation barrier. Hence, if the radius of the precipitate nuclei is less than a critical value, the precipitate phases cannot be nucleated. As a result, the quenching rate and section size considerably influences enlarge of hardening in precipitation strengthening.
c) The most significant advantage of spinodal hardening is that it is homogeneous throughout the section.
d) Easy melting and casting are used to build the modulated (spinodal) alloy as against the P/M method or internal oxidation to be used for dispersion strengthening.
e) At usual temperatures of application modulated (spinodal) alloys are not probable to over-age or recrystallize, while precipitation hardening alloys show a slow however exact over-ageing tendency.

3. EXPERIMENTAL RESEARCH

In this section, spinodal decomposition in copper, iron, titanium-based and other alloys will be summarized, as well as metallic glasses and polymers will be outlined in case of spinodal decomposition.

3.1 Spinodal decomposition in Cu-based alloys

A large number of investigators studied on Cu-Ni-Fe [4-5, 6, 7-11], Cu-Ni-Sn [3, 4, 12, 13-15, 16-17], Cu-Ni-Cr [18-19, 21,22, 23-25, 10, 26-28] and Cu based other alloys [29-31] using X-ray diffraction, transmission electron microscopy, electron diffraction, resistivity measurements and other techniques for example magnetic analysis and neutron diffraction.

a) Early stages of ageing

Various evidences of periodic decomposition products were detected in the electron micrographs of as quenched Cu-based specimens (Fig. 3*)*. In the early stages of aging, the characteristics of spinodal decomposition examined via XRD and electron microscopy are: (i) sidebands on the XRD peaks, (ii) periodic structure in the electron micrographs (Fig. 4), (iii) first aging connected with steady wavelength (Fig. 5), (iv) lack of any power of grain boundaries or dislocations on the decomposition [19, 23].

The volume fractions of the phases at ageing temperature were determined from tie lines constructed via X-ray energy dispersive chemical analysis of the phases in combination with the analyzed alloy compositions. For instance, the volume fraction of the copper depleted phase was 0.12 for the Cu-30Ni-5Cr alloy (wt-%), and 0.46 for the Cu-45Ni-l0Cr (wt-%) alloy at 800ºC [24,25].

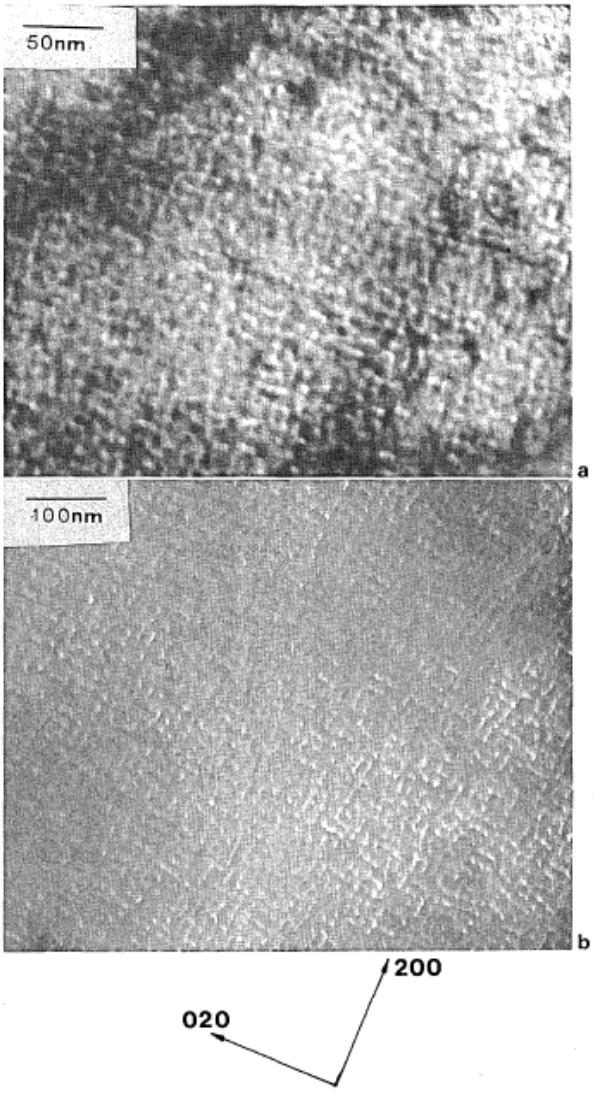

Figure 3 – Periodic structure in Cu-45Ni-10Cr alloy: λ≈8 nm (TEM), a) as quenched; b) aged 2 h at 300ºC [19]

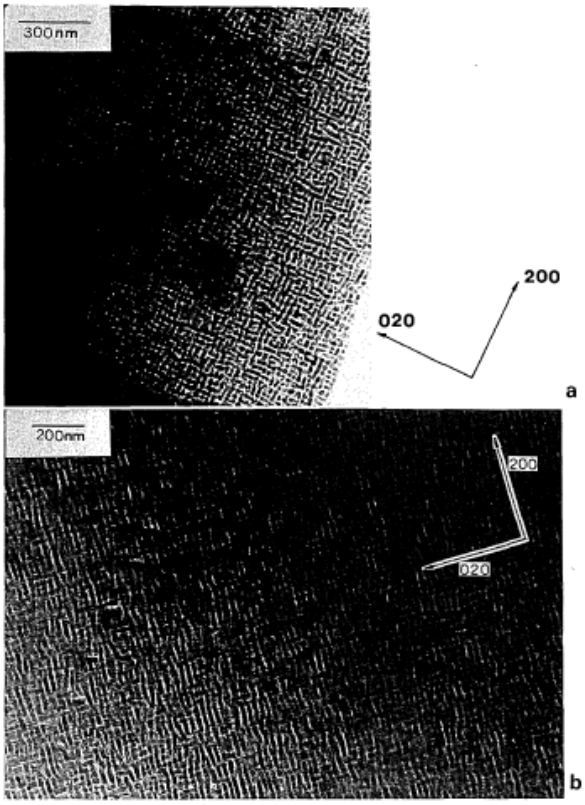

Figure 4 – Periodic structure in Cu-45Ni-10Cr alloy (TEM), a) aged 5 min, 800°C, λ≈16 nm; b) aged 1 day, 600°C, λ≈17 nm [19]

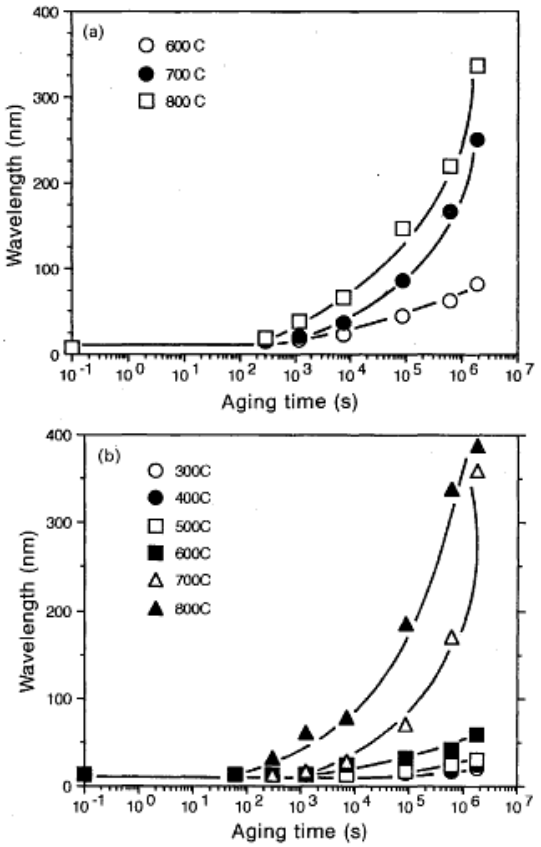

Figure 5 – Wavelength λ as function of aging time at various temperatures for a) Cu-30Ni-5Cr and b) Cu-45Ni-15Cr alloys [23]

In all Cu-based alloys for the period of the first stages of aging the particles were small, periodic, and cuboidal, and λ remained stable. Heterogeneous precipitation and precipitate free zones next to grain boundaries were not detected. Twin phases have all alloying elements and no pure phase was observed, in contrast to an earlier paper [32]. The particles clustered mutually and joined to shape periodic arrays of rods elongated in the <100> directions in both alloys as aging proceeded (Fig.4a). The precipitation characteristics detected are completely reliable with spinodal decomposition. After extended aging times at high temperatures, interfacial dislocations developed at the particles (Figs. 6b and 6c) and grain boundary precipitation was detected (Fig. 6d). The previous is proof of loss of coherency and is connected with a reduction in hardness in the aging curves (Fig. 7). Following extended aging, the coarsened structure contained platelets. The morphological progress on aging can be summarized as cuboids → rods → platelets. These results are in harmony with prior investigation [33,34].

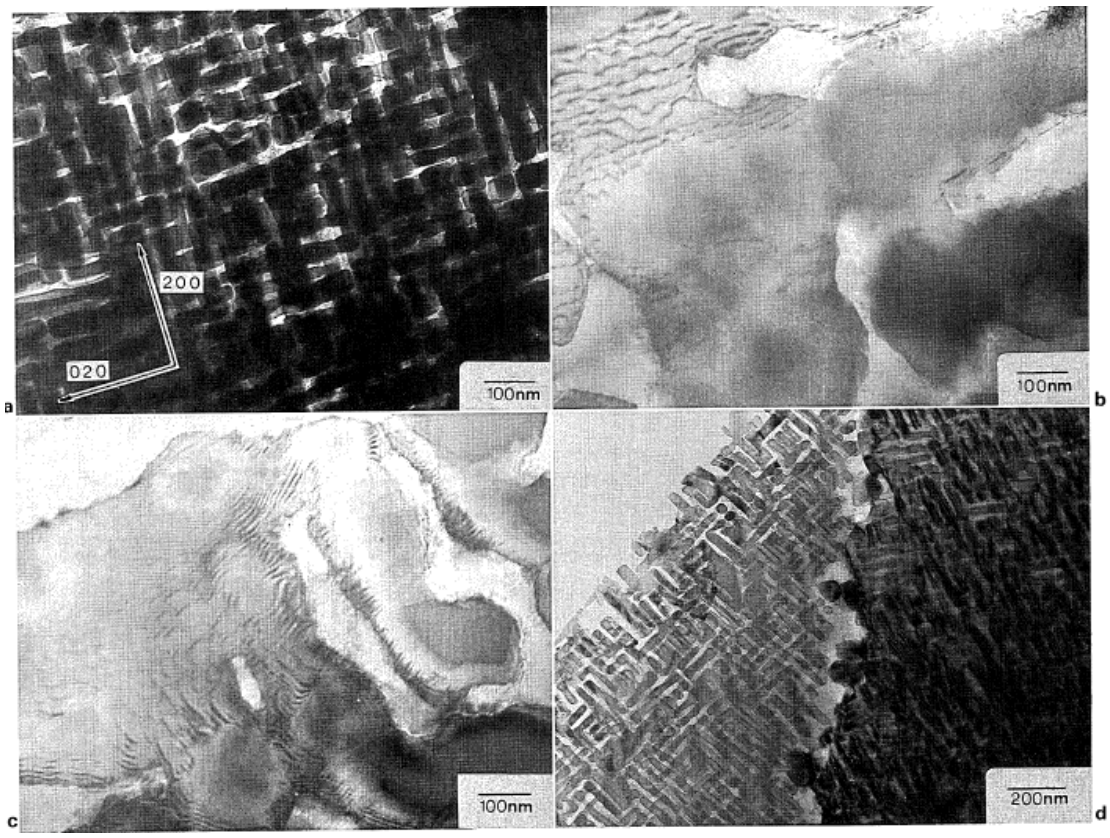

Figure 6 – Microstructure of Cu-45Ni-10Cr alloy following different aging treatments, a) feature spinodal decomposition structure after 3 weeks at 600°C, $\lambda \approx 40$ nm; b) interfacial dislocations after 1 week at 800°C, $\lambda \approx 330$ nm; c) coarse (platelet) structure after 1 week at 800°C, $\lambda \approx 330$ nm; d) grain boundary precipitation after 20 min at 800°C, $\lambda \approx 40$ nm [19]

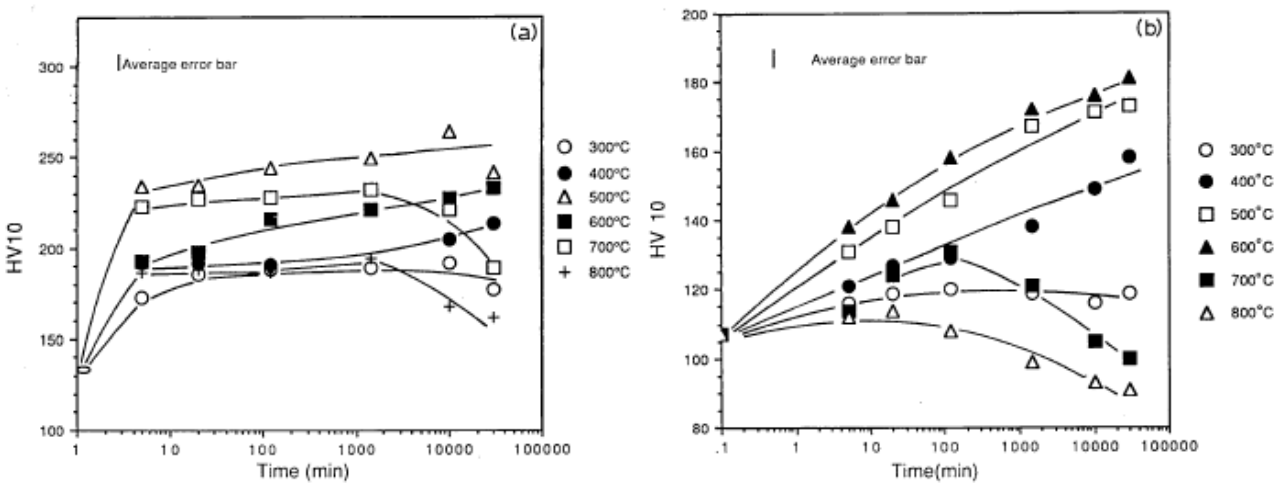

Figure 7 – Hardness (HV10) as function of aging time (min) for a) Cu-45Ni-10Cr and b) Cu-30Ni-2·5Cr alloy [19].

b) Later stages of ageing

In the Cu-based alloys, extended aging, particularly at higher temperatures resulted in the configuration of little spheroidal particles of a third phase (Fig. 8). Diffraction designated that these particles are bcc and, from EDX analysis, they were decided to be very rich in chromium. Their small dimension and the overlap of other phases in the thin foils excluded quantitative analysis although they seem to have some nickel and copper, opposing to an previous report of the formation of a 'pure chromium' phase [35]. In the Cu-45Ni-10Cr alloy, the microstructure of the decomposition products was not exaggerated by aging (Fig. 6d) and the cuboidal form stayed, even at the elevated aging temperatures. On the other hand, at 700 and 800°C, the cuboidal particle arrangement was uneven in distribution (e.g. Fig. 8*)* and sidebands were not observed on XRD patterns [19, 23]. By contrast, the cuboids firstly produced in the Cu-45Ni-10Cr alloy altered to rods aligned along (100) (Fig. 6a*)* and lastly to plates (Fig. 7b). This morphological change progression is in conformity with earlier reports [36, 33]. Loss of coherency and, progress of interfacial dislocation networks was also detected (Figs. 6b, 6c).

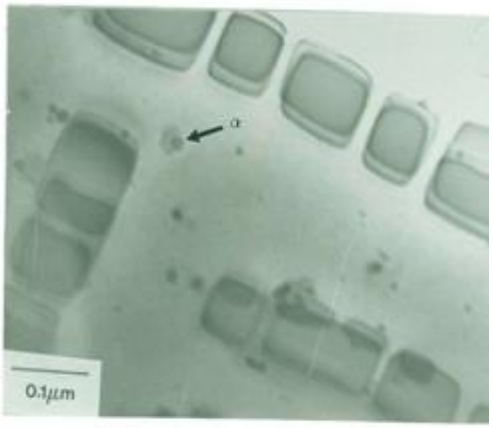

Figure 8– Electron micrographs of aged Cu-30Ni-5Cr alloy during the early stages of ageing. Structure lacks periodicity in all but 1 direction after 1 day ageing at 800°C, λ≈1600 Å [23]

Coarsening of the decomposition products was chased by measurement of the wavelength of the periodic structure as a function of aging temperature and time. The wavelength of decomposition was deliberated either directly from the enlarged micrographs (large λ) or by calculation of the sidebands on the XRD patterns via the Daniel-Lipson equation: the 200 peak was utilized for measurement since it gave the most excellent arrangement of intensity and sideband resolution. The pertinent coarsening equation is [32, 37, 38].

$$\lambda_t^n - \lambda_0^n = k(t - to) \qquad (4)$$

where λ_t is the wavelength of composition modulation at time *t*, λ_o is the first constant wavelength, *k* and *n* are constants, and *to* is the time at which coarsening begins.

The progress of wavelength with time and temperature for both alloys can be observed in Fig. 5. At inferior temperatures (300-500°C), measurement of the wavelengths was not easy, therefore these values are not incorporated in Fig. 5*a*. Also, in Cu-45Ni-15Cr alloy, wavelengths at 300 and 400°C were very comparable and consequently merely the values at 400°C are illustrated in Fig.5b. The coarsening performance of the Cu-45Ni-15Cr alloy determined from log λ-*log(t - to)* graphs (Fig. 5b) is in conformity with equation (2) while the exponent $n = 3$. For other values of *n* the fit to the data is less good. Nevertheless, the Cu-30Ni-5Cr alloy did not follow this coarsening law particularly at lower temperatures (600°C) [24,25].

It has been revealed above that for the Cu-45Ni-15Cr alloy $\lambda \propto (t - to)^{1/3}$. Conversely, this does not directly designate the association between wavelength and particle size. The relationship between mean particle size *p* and wavelength λ for mutually alloys is exposed in Fig. 9. The slopes of the curves give the relationship between *p* and λ as $p \approx 0{,}580\lambda$ for the 5%Cr alloy and $p \approx 0.631\lambda$ for the 15%Cr alloy [19,23]. These results are in conformity with preceding investigation [39]. From graphs of time required for *p* to reach a fixed value (represented by *In(t - to))* versus the inverse of temperature (Fig. 10), the subsequent estimated values of the activation energy for coarsening Q were obtained: 218 and 261 kJ mol^{-1} for the 5 and 15%Cr alloys correspondingly.

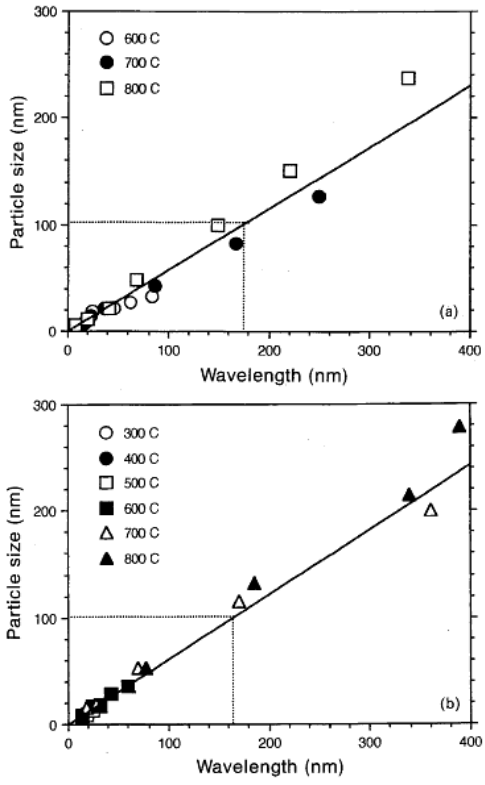

Figure 9 – Particle size as function of wavelength A for various aging temperatures in a) Cu-30Ni-5Cr and b) Cu-45Ni-15Cr alloys [23]

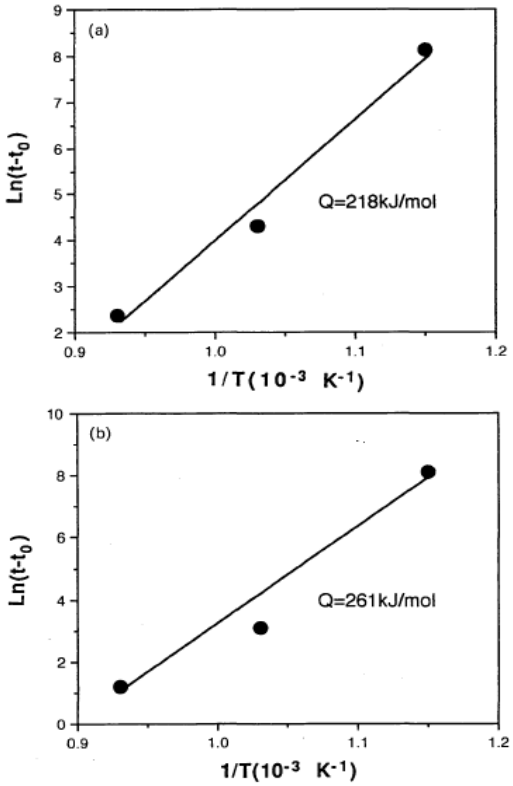

Figure 10 – Effect of temperature on time required to achieve particle size of a) 46 nm in Cu-30Ni-5Cr alloy and, b) 44 nm in Cu-45Ni-15Cr alloy [23]

Merely following extended aging times did precipitate free or denuded zones build up. This microstructural heterogeneity seems to derive chiefly from a comparatively fast loss of coherency of precipitate particles at grain boundaries and the special growth or coarsening of these particles at the expense of the coherent particles within the grains, as detected in earlier study [36].

The coarse precipitate structure and denuded area in the vicinity of the grain boundaries activate the migration of certain boundaries and a 'discontinuous coarsening' reaction finally involves the relocation of high angle grain boundaries and boundary diffusion, akin to cellular or discontinuous precipitation [36] (Fig. 12).

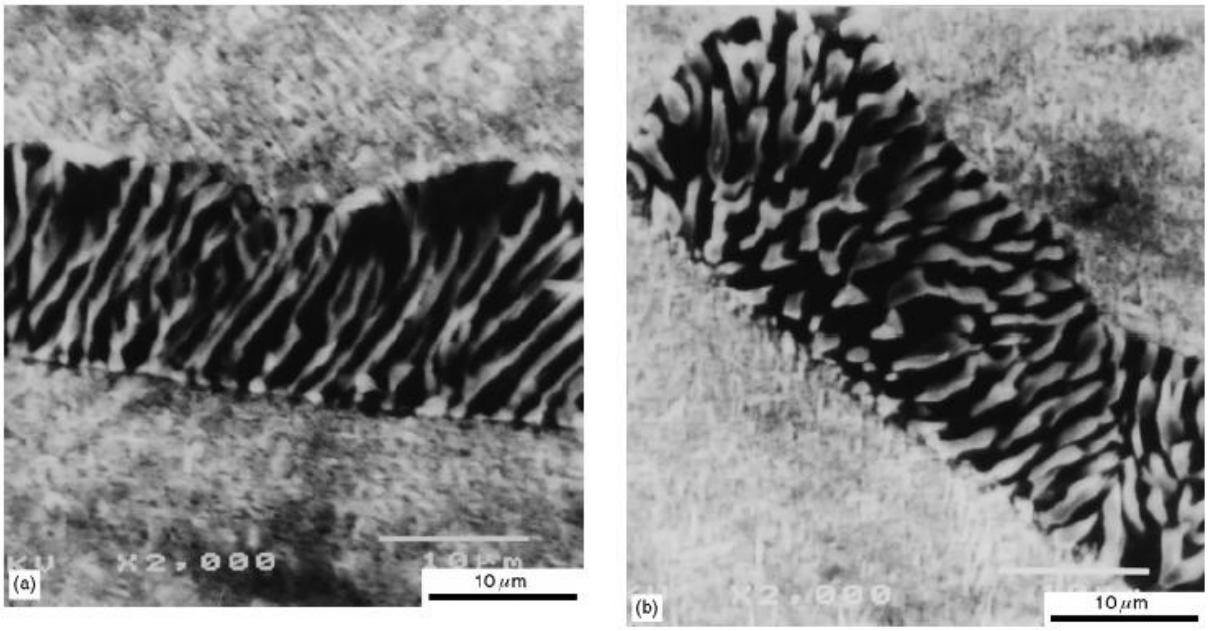

Figure 11– Scanning electron micrographs of different Cu-30Ni-5Cr alloys showing is continuous precipitation (2 h deep etched with Rosenthal's etchant). a) Discontinuous or cellular precipitation in C alloy after 3 weeks ageing at 700°C. b) Same as (a) but illustrating flake type structure (akin to tree branches) in the same alloy [40]

c) Age hardening

The hardness alteration was measured on specimens isothermally aged for diverse times in the temperature range 300-800°C and is exposed in Fig. 7. A very fast early rate of hardening can be observed in some Cu-based alloys (eg Cu-45Ni-10Cr in Fig. 7a), with an area showing a lower rate of hardening at longer times for all temperatures. The alteration from cuboids to rods was finished following very little aging times (~5 min) at 800°C, and the change from rods to platelets in 1 day, with a loss of coherency (Fig.6c). For temperatures in the range 300-600°C, hardness amplified continuously up to 10^5 min and a loss of coherency was not detected. Through this time, the precipitates distorted from cuboids to rods. At 700°C, the hardness curve illustrated a peak at ~100 min: coherency was preserved up to 1000 min at this temperature and subsequently loss of coherency started. Coarsening of the structure under these

conditions can be observed in Fig. 12. At this temperature (700°C) the morphological alteration progression can be printed as cuboids → rods within 1 day aging, and then rods →platelets.

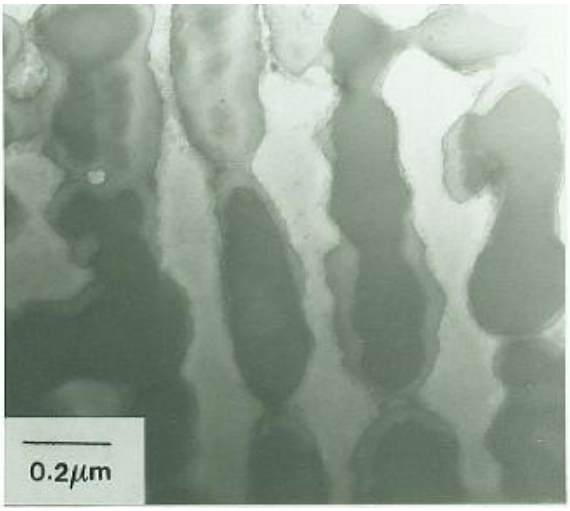

Figure 12 – Electron micrograph of Cu-45Ni-10Cr alloy during the later stages of ageing, showing more coarsened periodic structure (1 week aged at 800°C, λ≈3300Å) [19]

4. FUTURE DEVELOPMENTS

Spinodal alloys are compositionally neutral systems that show impetuous solute clustering on a nanoscale. This alteration occurs without a crystal structure change. Albeit spinodal decomposition was predicted by thermodynamics near the go round of the twentieth century, for a number of years, it was monitored only in ceramic systems. However, in the 1960s, with the beginning of TEM technology, spinodal decomposition was inspected in a number of alloy systems, counting the copper, iron and titanium alloys.

Right now, different spinodal alloys are intended for high strength applications, electrical and magnet alloys in addition to high speed cutting tools, for example cermets. For instance, today's copper–nickel–tin spinodal alloys are high performance wear resistant materials that function under arrangement of harsh load and speed. The outstanding characteristics of spinodal copper alloys have led to applications in large jet aircraft, highly difficult off-road equipment and heavy duty mechanical systems such as oilfield apparatus, which engages the extra advantage of corrosion resistance.

Alternatively, spinodal decomposition has been typically useful in the fabrication of stable magnet materials, because the morphologies favor high coercivities. The structure can be optimized by thermomechanical processing and magnetic aging. Permanent phase separation or spinodal decomposition appears to be important in the classic Alnicos and copper-nickel-iron alloys, as well as in the recently developed iron-chromium-cobalt materials.

Spinodal decomposition is usually utilized in manufacturing and their application area is revealed as follows:

1. In electrical, automobile and building industries.
2. In ordnance and also in biological and agricultural areas.
3. Condenser tubes and seawater piping.
4. Manufacture of bullet envelopes.
5. Coinage making.
6. Electrical resistance and thermocouples.
7. Turbine blades production.
8. Used to produce heat exchanger tubes.

In spite of the obtainable papers considered so far, the following issues still need to be investigated concerning spinodal decomposition:

(1)Novel alloying elements (such as high temperature elements ie Ti, Zr, Nb etc) can be added in order to delay the coarsening stage in the extended time ageing.

(2)Supplementary corrosion tests can be performed on spinodal alloys after short and long period ageing time.

(3)Wavelength-hardness connection can be compared to re-establish a universal hardening law for early and later ageing stages.

(4)Discontinuous (cellular) precipitation worsens good mechanical properties of spinodal alloys. Thus, to hold back or restrain the cellular precipitation in all alloys, trace elements (e.g. Al, Si, Mg) should be added to the copper-nickel-chromium ternary system.

(5)The bulk metallic glasses (BMG) have concerned great attention due to their exclusive properties and potential applications. Moreover many good properties, such as ultrahigh strength, good magnetic property, good anticorrosion property, and so on, they are also much cheaper in comparison to other BMGs.

(6) The potential applications of polymer solutions in dense or supercritical fluids and mixtures will prolong to be strong in arrangement of particles, porous materials, blends and fiber. There is a clear prominence on developments of materials with nanoscale features particularly for the biopharmaceutical or biomedical applications.

The heat treatment for modulated (spinodal) alloys was chiefly utilized to develop the mechanical properties of metallic alloys such as iron and copper ones. More lately the treatment has moved away from simple heat treatment and is utilized to create in marine applications such as the hulls of small ships, the cladding of rudders of large ocean going ships, sheathing in the splash zone of fixed offshore structures, desalination plant and associated pipe-work pumps, valves, instrumentation and control systems. Potential developments of the

process might produce advanced structures for the nuclear and aerospace industry.

5. CONCLUSIONS

Spinodal decomposition is a system by which a solution of two or more components can divide into separate phases with clearly dissimilar chemical compositions and physical properties. This system differs from classical nucleation in that phase separation owing to spinodal decomposition is much more delicate, and happens homogeneously throughout the material. The following conclusions can be drawn from the current investigation:

a. The spinodal reaction is a spontaneous unmixing or diffusional clustering dissimilar from classical nucleation and growth in metastable solutions. This different kinetic performance was explained earlier by Gibbs in his treatment of the thermodynamic stability of supersaturated phases.

b. Precipitation hardening, dispersion strengthening and spinodal decomposition methods provide roughly the same strength values. However there are compact advantageous of via spinodal decomposition method, such as homogeneous microstructure, no influencing by section thickness and uniform all over the section, as against the precipitation hardening method.

c. Various alloys such as Cu, Fe and Ti-based, metallic glasses and polymers rendering to spinodal decompositions. In the early stages of ageing, these alloys demonstrate (i) sidebands on the XRD peaks, (ii) periodic structure in the electron micrographs, and (iii) early aging associated with steady wavelength. In the later extended ageing times, coarsening and precipitate free or denuded zones expand.

6. ACKNOWLEDGEMENTS

Particular thanks are included to the Sakarya University and the International University of Sarajevo for financial support.

7. REFERENCES

[1] Soffa WA, Laughlin DE, in Solid-Solid Phase Transformations, Proceedings of an International Conference, Aaronson HI, Laughlin DE, Sekerka RF, Wayman CM, Ed., AIME, Warrendale, PA, 1982, p 159.

[2] Cahn JW. Spinodal decomposition, Trans. Met. Soc. AIME 1968; 242: 166-170.

[3] Abboud JH. MSc Thesis, Baghdad University, 1983.

[4] Ditchek B, Schwartz LH; Diffraction Study of Spinodal Decomposition In Cu-10 W-O Ni-6 W-O Sn, Acta Mater 1980; 28: 807-822.

[5] Butler EP, Thomas G. Structure and properties of spinodally decomposed Cu-Ni-Fe alloys, Proc R Soc 1970; 18: 347-351.

[6] Bouchard M, Livak RJ, Thomas G. Interphase interfaces in spinodal alloys, Surface Science 1972; 31: 275-295.

[7] Hargreaves ME. Side bands due to spinodal decomposition, Acta Cryst 1951; 4: 301-306.

[8] Hilert M, Cohen M, Averbach BL. Formation of modulated structures in copper-nickel-iron alloys, Acta Mater 1961; 9: 536-540.

[9] Cadoret R, Delavignette P. Ětude de la décomposition spinoïdale au microscope électronique dans les alliages CuNiFe, Phys Stat Sol 1969; 3: 853.

[10] Livak RJ, Thomas G. Spinodal Fe-Ni alloys, Phys Stat Sol 1971; 19: 497-504.

[11] Livak RJ. PhD Thesis, California University, Berkeley, Sept. 1972.

[12] Schwartz LH, Mahajan S, Plewes JT. Spinodal decomposition in a Fe-Cr alloys, Phys Stat Sol 1974; 22: 601-608.

[13] Schwartz LH, Plewes JT. High-strength Cu-Ni-Sn alloys by thermomechanical processing, Met Trans A 1974; 22: 911-917.

[14] Lefevre BG, D'annessa AT, Kalish D. Age hardening in Cu-15Ni-8Sn alloy, Met Trans A 1978; 9A: 577-582.

[15] Baburaj EG, Kulkarni UD, Menon ESK, Krishan R. Initial stages of decomposition in Cu-9Ni-6Sn, J Appl Cryst 1979; 12: 476-480.

[16] Leterrible P, Naudot P, Welter JM. Elaboration, properties, applications of Cu-Ni15-Sn8 hardened by spinodal decomposition, pp. 259-266, Copper Conference, October 1-3, 1990, Sweden.

[17] Virtanen P, Tiainen T. Effect of nickel content on the decomposition behavior and properties of CuNiSn alloys, Phs Stat Sol 1997; A159: 305-316.

[18] Findik F. Precipitation reactions in some Cu-Ni-Cr alloys, PhD Thesis, Imperial College, University of London, UK, 1992.

[19] Findik F, Flower HM. Microstructure and Hardness Development in Cu-30Ni-2.5Cr and Cu-45Ni-10Cr Spinodal Alloys, Materials Science and Technology 1992; 8: 197-205.

[20] Findik F. Side-Bands in Spinodal Cu-Ni-Cr Alloys and Lattice Parameter Inquiries, J Mater Sci Let 1993; 12: 338-342.

[21] Rao PP, Agrawal BK, Rao AM. Studies on spinodal decomposition in Cu-27Ni-2Cr alloy, J Mater Sci 1986; 21: 3759-3766.

[22] Rao PP, Agrawal BK, Rao AM. Comparative-study of spinodal decomposition in symmetrical and asymmetric Cu-Ni-Cr alloys, J Mater Sci 1991; 26: 1485-1496.

[23] Findik F, Flower HM. Morphological Changes and Hardness Evolution in Cu-30Ni-5Cr & Cu-45Ni-

15Cr Spinodal Alloys, Mater Sci & Techn 1993; 9: 408-416.
[24] Findik F. Particle Size-Wavelength Relationship and Ternary Diagram Inquiry in the Cu-Ni-Cr Ternary System, J Mater Sci 1993; 28: 5056-5059.
[25] Findik F. Modulated Structures in Cu-32Ni-3Cr and Cu-46Ni-17Cr Alloys, Canadian Metallurg Quart 2002; 41(3): 337-347.
[26] Meijering JL, Rathenau GW, Steeg MGVD, Braun PB. The miscibility gap in the Cu- Ni-Cr system, J Inst Met 1955; 84: 118-120.
[27] Meijering JL. Calculation of the nickel-chromium-copper phase diagram from binary data, Acta Met 1957; 5: 257-264.
[28] Manenc J. Diffusion anormale des rayons X au cours de la decomposition dans un groupe d'alliages Cu Ni Cr, Acta Met 1958; 6: 145-149.
[29] Lei Q, Li Z. et al. The evolution microstructure in Cu-8Ni-1.8Si-0.15Mg alloy during ageing, Mater Sci Eng A 2010; 527: 6728-6733.
[30] Yu Y, Wang C. et al. Direct evidence of fcc-type miscibility gap in the Cu-Ni-V system at high temperatures, Materials Letters 2011; 65: 247-249.
[31] Priya S, Jacob KT. Activities and immiscibility in the system Cu-Rh, J Phase Equilibria 2000; 21: 342-349.
[32] Metals Handbook, V. 8, p. 184, Ed. T. Lyman, ASM 1967.
[33] Avner SH. Introduction to Physical Metallurgy, Mc Graw Hill, New York, 1974, pp 461-480.
[34] Cahn JW. A correction to spinodal decomposition in cubic crystals, Acta Met 1962; 10: 179-183.
[35] Lane PHR, Huskins JC. in Marine Engineering with Cu-Ni, p. 59, Institute of Metals, London 1988.
[36] Badia FA, Kirkby GN, Mihalisin JR. Strengthening of Annealed Cupro-Nickels, ASM 1967; 60: 395-400.
[37] Hilliard JE. p. 501 in Phase Transformations, Ed. Aaronson HI, ASM 1970.
[38] Jack DH, Nutting J. Phase transformations, Int Met Rev 1974; 19: 90-104.
[39] Gronpsky R. MSc Thesis, Univ. of California, 1974.
[40] Findik F. Discontinuous (Cellular) Precipitation, J Mater Sci Let 1998; 17: 79-83.